

 Open access • Journal Article • DOI:10.1021/ES00160A010

## **Chromate adsorption on amorphous iron oxyhydroxide in the presence of major groundwater ions. — [Source link](#)**

John M. Zachara, Donald C. Girvin, R.L. Schmidt, C. T. Resch





**Institutions:** Pacific Northwest National Laboratory

**Published on:** 01 Jun 1987 - Environmental Science & Technology (American Chemical Society)

**Topics:** Adsorption and Chromate conversion coating

Related papers:

- [Adsorption of Chromate by Subsurface Soil Horizons](#)
- [Surface Complexation Modeling: Hydrated Ferric Oxide](#)
- [Chromate removal from aqueous wastes by reduction with ferrous ion](#)
- [Surface ionization and complexation at the oxide/water interface. 3. Adsorption of anions](#)
- [Chromium\(III\) hydrolysis constants and solubility of chromium\(III\) hydroxide](#)

Share this paper:    

View more about this paper here: <https://typeset.io/papers/chromate-adsorption-on-amorphous-iron-oxyhydroxide-in-the-85r5p413bn>

University of Nebraska - Lincoln

DigitalCommons@University of Nebraska - Lincoln

---

US Department of Energy Publications

U.S. Department of Energy

---

1987

## Chromate Adsorption on Amorphous Iron Oxyhydroxide in the Presence of Major Groundwater Ions

John M. Zachara

*Pacific Northwest National Laboratory, john.zachara@pnl.gov*

Donald Girvin

*Pacific Northwest National Laboratory*

Ronald Schmidt

*Pacific Northwest National Laboratory*

C. Thomas Resch

*Pacific Northwest National Laboratory*

Follow this and additional works at: <https://digitalcommons.unl.edu/usdoepub>



Part of the [Bioresource and Agricultural Engineering Commons](#)

---

Zachara, John M.; Girvin, Donald; Schmidt, Ronald; and Resch, C. Thomas, "Chromate Adsorption on Amorphous Iron Oxyhydroxide in the Presence of Major Groundwater Ions" (1987). *US Department of Energy Publications*. 204.

<https://digitalcommons.unl.edu/usdoepub/204>

This Article is brought to you for free and open access by the U.S. Department of Energy at DigitalCommons@University of Nebraska - Lincoln. It has been accepted for inclusion in US Department of Energy Publications by an authorized administrator of DigitalCommons@University of Nebraska - Lincoln.

# Chromate Adsorption on Amorphous Iron Oxyhydroxide in the Presence of Major Groundwater Ions

John M. Zachara,\* Donald C. Girvin, Ronald L. Schmidt, and C. Thomas Resch

Battelle, Pacific Northwest Laboratories, Richland, Washington 99352

■ Chromate adsorption on amorphous iron oxyhydroxide was investigated in dilute iron suspensions as a single solute and in solutions of increasing complexity containing  $\text{CO}_2(\text{g})$ ,  $\text{SO}_4^{2-}(\text{aq})$ ,  $\text{H}_4\text{SiO}_4(\text{aq})$ , and cations [ $\text{K}^+$ ,  $\text{Mg}^{2+}$ ,  $\text{Ca}^{2+}(\text{aq})$ ]. In paired-solute systems (e.g.,  $\text{CrO}_4^{2-}$ - $\text{H}_2\text{CO}_3^*$ ), anionic cosolutes markedly reduce  $\text{CrO}_4^{2-}$  adsorption through a combination of competitive and electrostatic effects, but cations exert no appreciable influence. Additionally,  $\text{H}_4\text{SiO}_4$  exhibits a strong time-dependent effect:  $\text{CrO}_4^{2-}$  adsorption is greatly decreased with increasing  $\text{H}_4\text{SiO}_4$  contact time. In multiple-ion mixtures, each anion added to the mixture decreases  $\text{CrO}_4^{2-}$  adsorption further. Adsorption constants for the individual reactive solutes were used in the triple-layer model. The model calculations are in good agreement with the  $\text{CrO}_4^{2-}$  adsorption data for paired- and multiple-solute systems. However, the model calculations underestimate  $\text{CrO}_4^{2-}$  adsorption when surface site saturation is approached. Questions remain regarding the surface interactions of both  $\text{CO}_2(\text{aq})$  and  $\text{H}_4\text{SiO}_4$ . The results have major implications for the adsorption behavior of  $\text{CrO}_4^{2-}$  and other oxyanions in subsurface waters.

## Introduction

Hexavalent chromium ( $\text{CrO}_4^{2-}$ ) is an antibiofoulant and anticorrosive agent and is common in industrial wastewaters. Dissolved  $\text{CrO}_4^{2-}$  is toxic to many organisms at low aqueous concentration (1) and is a regulated constituent in domestic water supplies (2). Chromate-containing wastes are often disposed of to the land surface or, as part of a complex aqueous solute mixture, to waste ponds or lagoons. These practices lead to concern over  $\text{CrO}_4^{2-}$  migration to and within nearby groundwaters.

Mineral phases with proton-specific surface sites, particularly those with high zero points of charge (e.g., iron and aluminum oxides), may effectively adsorb  $\text{CrO}_4^{2-}$  from pH 2 to pH 7 (3-7). Like other weak acid oxyanions (e.g.,  $\text{SeO}_4^{2-}$ ,  $\text{SO}_4^{2-}$ , and  $\text{AsO}_4^{3-}$ ),  $\text{CrO}_4^{2-}$  adsorption is pH dependent on these adsorbents, reflecting the charging of the adsorbent surface and solute speciation. Amorphous iron oxide [ $\text{Fe}_2\text{O}_3 \cdot \text{H}_2\text{O}(\text{am})$ ] or ferrihydrite, a common surface coating of subsoil particles, has a particularly high capacity for Cr(VI), reaching 0.1 mol of Cr/mol of Fe at a solution pH of <5.5 (5). This capacity reflects the high surface area and site density of  $\text{Fe}_2\text{O}_3 \cdot \text{H}_2\text{O}(\text{am})$ .

Despite the strong adsorption affinity of  $\text{CrO}_4^{2-}$  for certain proton-specific mineral surfaces, it is mobile in soil and subsurface systems (8-10). The presence of other competing anions may reduce  $\text{CrO}_4^{2-}$  adsorption and thus increase its mobility. Preliminary evidence suggests that solute interactions may be significant. Cosorption of  $\text{SO}_4^{2-}$  on  $\text{Fe}_2\text{O}_3 \cdot \text{H}_2\text{O}(\text{am})$  reduces  $\text{CrO}_4^{2-}$  adsorption by as much as 80% (5). Phosphate and selenite compete on goethite (11). Similarly, a ligand-exchange model suggests that anion adsorption on goethite in natural lakewater is largely controlled by silicate and phosphate sorption, which influence adsorbent surface speciation and charge (12, 13). These limited observations and the wide range of inorganic ions ranging up to  $10^{-2}$  M in natural waters suggest the need for improved understanding of  $\text{CrO}_4^{2-}$  adsorption from complex solute mixtures.

This paper reports the adsorption of  $\text{CrO}_4^{2-}$  at typical environmental concentrations on  $\text{Fe}_2\text{O}_3 \cdot \text{H}_2\text{O}(\text{am})$  in the presence of common cations and anions present in groundwater ( $\text{K}^+$ ,  $\text{Mg}^{2+}$ ,  $\text{Ca}^{2+}$ ,  $\text{SO}_4^{2-}$ ,  $\text{CO}_2(\text{aq})$ ,  $\text{H}_4\text{SiO}_4$ ). Single-solute equilibrium adsorption constants for  $\text{CrO}_4^{2-}$ ,  $\text{SO}_4^{2-}$ ,  $\text{Ca}^{2+}$ ,  $\text{CO}_2(\text{aq})$ ,  $\text{Na}^+$ , and  $\text{NO}_3^-$  derived under  $\text{N}_2(\text{g})$  atmosphere are used in the triple-layer adsorption model (TLM) (14) to simulate  $\text{CrO}_4^{2-}$  adsorption in the presence of single and multiple interacting ions.

## Experimental Procedures

**Synthesis of  $\text{Fe}_2\text{O}_3 \cdot \text{H}_2\text{O}(\text{am})$ .** Amorphous iron oxide [ $\text{Fe}_2\text{O}_3 \cdot \text{H}_2\text{O}(\text{am})$ ] was prepared in a jacketed reaction flask (at 25 °C) by hydrolysis of a sparged 0.1 M  $\text{Fe}(\text{NO}_3)_3$  solution. An automatic titration system was used to add the base [1.0 M NaOH,  $\text{CO}_2(\text{g})$ -free as determined by analysis] at a constant rate up to pH 7.25. Carbonate-free conditions were maintained during precipitation by using a glovebox with  $\text{N}_2$  atmosphere or, more commonly, by using a partially sealed reaction flask with continuous  $\text{N}_2$  sparge to prevent air intrusion. The suspension was allowed to equilibrate under  $\text{N}_2$  atmosphere (25 °C) for 14 h before use.

**Adsorption Experiments. (A) Basic Procedure.** Adsorption experiments were conducted in a jacketed 500-mL reaction flask that had been "presaturated" with Cr(VI) to eliminate potential adsorption by the flask during the experiment. The temperature was kept constant (at 25 °C) with a recirculating water bath. The  $\text{Fe}_2\text{O}_3 \cdot \text{H}_2\text{O}(\text{am})$  suspension was placed in the reaction vessel with an electrolyte (0.1 M  $\text{NaNO}_3$ ) and equilibrated (1 h) under  $\text{N}_2$  atmosphere at pH 9.0-9.5 where no sorption was anticipated, after which time the appropriate solutes and  $^{51}\text{Cr}$  (approximately 5000 cpm/mL) were added. An aliquot was immediately removed as a counting standard for the adsorbate, and the pH of the suspension was incrementally adjusted downward. Duplicate samples of the suspensions were removed at the desired pH levels, placed in  $\text{N}_2$ -sparged Corex (Corning Glass Works, Houghton Park, NY) centrifuge tubes (35 mL), and shaken for 4 h in a controlled-environment shaker ( $\text{N}_2$  atmosphere, 25 °C). The final pH was then measured in stirred suspensions under  $\text{N}_2$  atmosphere with a Ross combination pH electrode, and aliquots of the supernate were analyzed. The activity of  $^{51}\text{Cr}$  was determined by a Packard  $\gamma$  spectrophotometer with an NaI well crystal. The quantity adsorbed was the difference between the initial and final concentrations.

**(B) Single- and Paired-Solute Adsorption.** Chromate adsorption ( $5.0 \times 10^{-6}$  M) was measured at  $0.87 \times 10^{-3}$  and  $17.4 \times 10^{-3}$  M total iron. Inorganic carbon adsorption ( $[\text{C}_T] = 4.6 \times 10^{-6}$  M) was measured in similar iron suspensions spiked with  $\text{NaHCO}_3$ - $\text{NaH}^{14}\text{CO}_3$  over a pH range of 5.5-9. The tightly sealed individual centrifuge tubes with zero headspace stood for 24 h before carbonate adsorption was measured by  $^{14}\text{C}$  scintillation counting of  $^{14}\text{C}$ . The constancy of  $[\text{C}_T]$  was confirmed by directly analyzing some samples for total inorganic carbon.

Chromate adsorption in the presence of  $\text{CO}_2(\text{g})$  was investigated in a glovebox filled with a  $\text{CO}_2/\text{N}_2$  mixture containing  $P_{\text{CO}_2} = 10^{-2.46}$  atm. The 350-mL suspensions

**Table I. Triple-Layer Model Parameters for Fe<sub>2</sub>O<sub>3</sub>•H<sub>2</sub>O(am) Used in This Study**

surface site density ( <i>N<sub>s</sub></i> ) <sup>a</sup>	11 sites/nm <sup>2</sup> (9.8 mmol of sites/g Fe)
surface area ( <i>S</i> ) <sup>b</sup>	600 m <sup>2</sup> /g
outer-layer capacitance ( <i>C<sub>2</sub></i> ) <sup>a</sup>	0.20 F/m <sup>2</sup>
inner-layer capacitance ( <i>C<sub>1</sub></i> ) <sup>b</sup>	1.25 F/m <sup>2</sup>

<sup>a</sup> Davis et al. (14). <sup>b</sup> Girvin et al. (15).

**Table II. Surface Complexation Reactions and Triple-Layer Model Constants for Fe<sub>2</sub>O<sub>3</sub>•H<sub>2</sub>O(am)**

	reactions	constants
1	SOH <sub>2</sub> <sup>+</sup> ⇌ SOH + H <sup>+</sup>	log <i>K</i> <sub>al</sub> = -5.4 <sup>a</sup>
2	SOH ⇌ SO <sup>-</sup> + H <sup>+</sup>	log <i>K</i> <sub>a2</sub> = -10.3 <sup>a</sup>
3	SOH + Na <sup>+</sup> ⇌ (SO <sup>-</sup> -Na <sup>+</sup> ) <sup>0</sup> + H <sup>+</sup>	log * <i>K</i> <sub>Na</sub> = -8.6 (1.7) <sup>a,b</sup>
4	SOH + NO <sub>3</sub> <sup>-</sup> + H <sup>+</sup> ⇌ (SOH <sub>2</sub> <sup>+</sup> -NO <sub>3</sub> <sup>-</sup> ) <sup>0</sup>	log * <i>K</i> <sub>NO<sub>3</sub></sub> = 7.5 (2.1) <sup>a,b</sup>
5	SOH + CO <sub>3</sub> <sup>2-</sup> + 2H <sup>+</sup> ⇌ (SOH <sub>2</sub> <sup>+</sup> -HCO <sub>3</sub> <sup>-</sup> ) <sup>0</sup>	log * <i>K</i> <sub>HCO<sub>3</sub></sub> = 20.7 (5.0) <sup>b</sup>
6	SOH + CO <sub>3</sub> <sup>2-</sup> + 2H <sup>+</sup> ⇌ (SOH-H <sub>2</sub> CO <sub>3</sub> <sup>*</sup> ) <sup>0</sup>	log * <i>K</i> <sub>H<sub>2</sub>CO<sub>3</sub></sub> <sup>*</sup> = 20.0 (3.2) <sup>b,c</sup>
7	SOH + CrO <sub>4</sub> <sup>2-</sup> + H <sup>+</sup> ⇌ (SOH <sub>2</sub> <sup>+</sup> -CrO <sub>4</sub> <sup>2-</sup> ) <sup>-</sup>	log * <i>K</i> <sub>CrO<sub>4</sub></sub> = 10.1 (4.7) <sup>b</sup>
8	SOH + CrO <sub>4</sub> <sup>2-</sup> + 2H <sup>+</sup> ⇌ (SOH <sub>2</sub> <sup>+</sup> -HCrO <sub>4</sub> <sup>-</sup> ) <sup>0</sup>	log * <i>K</i> <sub>HCrO<sub>4</sub></sub> = 19.3 (7.5) <sup>b</sup>
9	SOH + SO <sub>4</sub> <sup>2-</sup> + H <sup>+</sup> ⇌ (SOH <sub>2</sub> <sup>+</sup> -SO <sub>4</sub> <sup>2-</sup> ) <sup>-</sup>	log * <i>K</i> <sub>SO<sub>4</sub></sub> = 11.6 (6.2) <sup>b</sup>
10	SOH + SO <sub>4</sub> <sup>2-</sup> + 2H <sup>+</sup> ⇌ (SOH <sub>2</sub> <sup>+</sup> -HSO <sub>4</sub> <sup>-</sup> ) <sup>0</sup>	log * <i>K</i> <sub>HSO<sub>4</sub></sub> = 17.3 (10.0) <sup>b</sup>
11	SOH + Ca <sup>2+</sup> ⇌ (SO <sup>-</sup> -Ca <sup>2+</sup> ) <sup>+</sup> + H <sup>+</sup>	log * <i>K</i> <sub>Ca</sub> = -6.3 (4.0) <sup>b</sup>

<sup>a</sup> Constants derived in Girvin et al. (15). <sup>b</sup> The log *K* values in parentheses correspond to adsorption reactions for which hydrolysis reactions for the adsorbing species and/or surface ionization reactions have been subtracted out. <sup>c</sup> Like the convention used for aqueous solutions [H<sub>2</sub>CO<sub>3</sub><sup>\*</sup> = H<sub>2</sub>CO<sub>3</sub> + CO<sub>2</sub>(aq) (17)], SOH-H<sub>2</sub>CO<sub>3</sub><sup>\*</sup> suggests that the surface complex consists of a mixture of the species SOH-H<sub>2</sub>CO<sub>3</sub> and SOH-CO<sub>2</sub>(aq), which are experimentally indistinguishable. In keeping with this definition, reaction 6 may be expressed equivalently as SOH + CO<sub>3</sub><sup>2-</sup> + 2H<sup>+</sup> ⇌ SOH-CO<sub>2</sub>(aq) + H<sub>2</sub>O [\**K*<sub>CO<sub>2</sub>(aq)</sub>].

of Fe<sub>2</sub>O<sub>3</sub>•H<sub>2</sub>O(am) were adjusted with acid and base to the desired pH and allowed to equilibrate for 4 h with CO<sub>2</sub>(g). Solution analysis for inorganic C verified equilibrium with *P*<sub>CO<sub>2</sub></sub> = 10<sup>-2.46</sup> atm. Chromate (5.0 × 10<sup>-6</sup> M) was added to each of the suspensions, which were stirred, open to the atmosphere, for 4 h. After this period, the final pH was measured, and replicate aliquots were removed from each suspension for CrO<sub>4</sub><sup>2-</sup> analysis.

The influence of H<sub>4</sub>SiO<sub>4</sub> (0.8 × 10<sup>-3</sup> M) on CrO<sub>4</sub><sup>2-</sup> adsorption was evaluated as a function of H<sub>4</sub>SiO<sub>4</sub> contact time with Fe<sub>2</sub>O<sub>3</sub>•H<sub>2</sub>O(am). Silicic acid was prepared by basic hydrolysis of sodium metasilicate (Na<sub>2</sub>SiO<sub>3</sub>•9H<sub>2</sub>O). The silica stock solution was 1.0 M in concentration with a pH > 13. The degree of silica polymerization in the stock solution was not evaluated. The influence of the simultaneous cosorption of H<sub>4</sub>SiO<sub>4</sub> on CrO<sub>4</sub><sup>2-</sup> was determined by spiking an Fe<sub>2</sub>O<sub>3</sub>•H<sub>2</sub>O(am) suspension (aged ~14 h) with the two ions simultaneously and immediately measuring the adsorption edge. Subsequently, individual aliquots of freshly prepared iron suspension were allowed to age at pH 7 in the presence of the same concentration of H<sub>4</sub>SiO<sub>4</sub> for 24, 168, and 672 h under N<sub>2</sub>. After aging, the suspension pH was adjusted back up to pH 10, and a typical adsorption experiment was conducted after the addition of CrO<sub>4</sub><sup>2-</sup> and <sup>61</sup>CrO<sub>4</sub><sup>2-</sup>.

In the cation experiments the basic adsorption procedure was followed, but 5.0 × 10<sup>-3</sup> M K<sup>+</sup>, Mg<sup>2+</sup>, and Ca<sup>2+</sup> were

**Table III. Aqueous Speciation Reactions and Equilibrium Constants**

	reaction	log <i>K</i> <sup>a</sup>
1	H <sup>+</sup> + SO <sub>4</sub> <sup>2-</sup> ⇌ HSO <sub>4</sub> <sup>-</sup>	1.99
2	Na <sup>+</sup> + SO <sub>4</sub> <sup>2-</sup> ⇌ NaSO <sub>4</sub> <sup>-</sup>	0.70
3	H <sup>+</sup> + CrO <sub>4</sub> <sup>2-</sup> ⇌ HCrO <sub>4</sub> <sup>-</sup>	6.51 <sup>b</sup>
4	2H <sup>+</sup> + CrO <sub>4</sub> <sup>2-</sup> ⇌ H <sub>2</sub> CrO <sub>4</sub>	5.56 <sup>c</sup>
5	Na <sup>+</sup> + CrO <sub>4</sub> <sup>2-</sup> ⇌ NaCrO <sub>4</sub> <sup>-</sup>	0.70 <sup>c</sup>
6	2H <sup>+</sup> + 2CrO <sub>4</sub> <sup>2-</sup> ⇌ Cr <sub>2</sub> O <sub>7</sub> <sup>2-</sup> + H <sub>2</sub> O	14.56 <sup>c</sup>
7	2H <sup>+</sup> + CO <sub>3</sub> <sup>2-</sup> ⇌ H <sub>2</sub> CO <sub>3</sub>	16.68
8	H <sup>+</sup> + CO <sub>3</sub> <sup>2-</sup> ⇌ HCO <sub>3</sub> <sup>-</sup>	10.33
9	Na <sup>+</sup> + H <sup>+</sup> + CO <sub>3</sub> <sup>2-</sup> ⇌ NaHCO <sub>3</sub> <sup>0</sup>	10.08
10	Na <sup>+</sup> + CO <sub>3</sub> <sup>2-</sup> ⇌ NaCO <sub>3</sub> <sup>-</sup>	1.27
11	Ca <sup>2+</sup> + H <sub>2</sub> O ⇌ CaOH <sup>+</sup> + H <sup>+</sup>	-12.60
12	Ca <sup>2+</sup> + SO <sub>4</sub> <sup>2-</sup> ⇌ CaSO <sub>4</sub> <sup>0</sup>	2.31
13	Ca <sup>2+</sup> + H <sup>+</sup> + CO <sub>3</sub> <sup>2-</sup> ⇌ CaHCO <sub>3</sub> <sup>+</sup>	11.33
14	Ca <sup>2+</sup> + CO <sub>3</sub> <sup>2-</sup> ⇌ CaCO <sub>3</sub> <sup>0</sup>	3.15

<sup>a</sup> From Truesdell and Jones, Ball, Nordstrom, and Jenne, and Ball, Jenne, and Cantrell (18–20) and Krupka and Jenne (21). <sup>b</sup> Baes and Mesmer (22). <sup>c</sup> Schmidt (23).

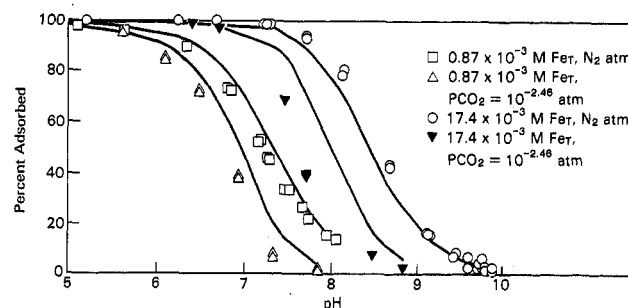


**Figure 1.** Fractional adsorption of 5.0 × 10<sup>-6</sup> M CrO<sub>4</sub><sup>2-</sup> on Fe<sub>2</sub>O<sub>3</sub>•H<sub>2</sub>O(am) in 0.1 M NaNO<sub>3</sub>. Experimental data points are shown by symbols. The solid curves were calculated from the model defined in Tables I–III; the adjustable parameters for the model were determined from the data represented by the open squares and open circles.

added to Fe<sub>2</sub>O<sub>3</sub>•H<sub>2</sub>O(am) suspensions individually as the nitrate salt immediately preceding the addition of chromate.

**(C) Multiple-Solute Adsorption.** Chromate (5.0 × 10<sup>-6</sup> M) adsorption on Fe<sub>2</sub>O<sub>3</sub>•H<sub>2</sub>O(am) was investigated from two multiple-solute mixtures: (1) 2.5 × 10<sup>-3</sup> M CaSO<sub>4</sub>(aq) and *P*<sub>CO<sub>2</sub></sub> = 10<sup>-2.46</sup> atm and (2) 2.5 × 10<sup>-3</sup> M CaSO<sub>4</sub>(aq), *P*<sub>CO<sub>2</sub></sub> = 10<sup>-2.46</sup> atm, and 8.0 × 10<sup>-4</sup> M H<sub>4</sub>SiO<sub>4</sub>. The experiments were performed as described above for the CrO<sub>4</sub><sup>2-</sup>-CO<sub>2</sub>(g) system, except that CaSO<sub>4</sub>(aq) and H<sub>4</sub>SiO<sub>4</sub> were added immediately preceding CrO<sub>4</sub><sup>2-</sup>.

**(D) Modeling of Adsorption Data.** The triple-layer model (TLM) (14) has been used to simulate the adsorption data. The TLM parameters for Fe<sub>2</sub>O<sub>3</sub>•H<sub>2</sub>O(am) are listed in Table I. Surface hydrolysis and complexation of the supporting electrolyte (NaNO<sub>3</sub>) are described by reactions 1–4 in Table II. The equilibrium constants for these reactions were derived from potentiometric titration data for Fe<sub>2</sub>O<sub>3</sub>•H<sub>2</sub>O(am) (15). Surface complexation reactions 5–11 (Table II) have been used to describe the adsorption data presented below. The equilibrium constants for these reactions have been derived from single- or paired-solute adsorption data with FITEQL (16) and the aqueous speciation reactions in Table III. These constants have in turn been used to simulate multiple-solute adsorption data. It has been assumed throughout that all adsorbing ions interact with a single set of surface sites, SOH.

## Results and Discussion

**Single-Solute Adsorption of Inorganic Carbon on Fe<sub>2</sub>O<sub>3</sub>•H<sub>2</sub>O(am).** The presence of CO<sub>2</sub>(g) (*P*<sub>CO<sub>2</sub></sub> = 10<sup>-2.46</sup>

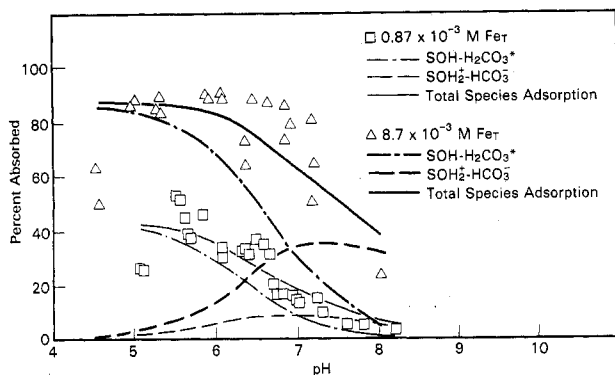
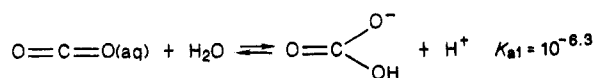


**Figure 2.** Closed-system adsorption of carbonate species ( $[C_T] = 4.6 \times 10^{-6}$  M) on  $\text{Fe}_2\text{O}_3 \cdot \text{H}_2\text{O}(\text{am})$  in 0.1 M  $\text{NaNO}_3$ . Data points are shown by symbols, and solid and dashed curves represent the optimum fit for total and individual species adsorption, respectively.

atm) moves the  $\text{CrO}_4^{2-}$  adsorption edge to lower pH relative to that obtained under  $\text{N}_2$  atmosphere (Figure 1). This effect of  $\text{CO}_2(\text{g})$  suggests that aqueous carbonate species are adsorbed and that they influence  $\text{CrO}_4^{2-}$  adsorption via electrostatic interactions or competitive mass action for surface sites (SOH).

The measurement of  $^{14}\text{C}$  removal from  $^{14}\text{C}$ -labeled  $\text{NaHCO}_3$  solutions provides direct evidence for the adsorption of aqueous carbonate species by  $\text{Fe}_2\text{O}_3 \cdot \text{H}_2\text{O}(\text{am})$  (Figure 2). An adsorption maximum occurs in the region of the  $\text{p}K_{a1}(\text{H}_2\text{CO}_3^*) = 6.3$ , a positioning that is similar to that observed for  $\text{H}_3\text{BO}_3$  and  $\text{H}_4\text{SiO}_4$  (24, 13). The phenomenon differs, however, because  $\text{H}_2\text{CO}_3^* [= \text{CO}_2(\text{aq}) + \text{H}_2\text{CO}_3]$  is a stronger acid, exists primarily as  $\text{CO}_2(\text{aq})$  ( $\sim 99\%$  at  $25^\circ\text{C}$ ), and undergoes a change in structure as given by the combined hydration and dissociation reaction:



The adsorption of inorganic carbon species (Figure 2) can be described with the TLM by reactions 5 and 6 (Table II). The adsorption constants for these reactions  $*K_{\text{HCO}_3^-}$  and  $*K_{\text{H}_2\text{CO}_3^*}$  (Table II) were derived from both sets of data in Figure 2 with FITZQL. Reactions 5 and 6 qualitatively reproduce the increase in inorganic carbon adsorption from pH 8 to pH 5.5. They fail, however, to predict the decline that is suggested by the sparse experimental data below pH 5.5. Neither reaction 5 nor reaction 6 alone could adequately describe both the 0.87 and 8.7 mM  $\text{Fe}_T$  data. Inclusion of a reaction yielding  $\text{SOH}_2^+ - \text{CO}_3^{2-}$  with reactions 5 and 6 did not improve the fit because no data above pH 8 were obtained where this species might dominate. The Boltzmann factors for  $\text{H}^+$  and  $\text{CO}_3^{2-}$  ions in the TLM that describe the electrostatic interaction between the ions and the charged surface cancel in reaction 6. Thus, the location of the  $\text{H}_2\text{CO}_3^*$  surface complex is not specified within the context of the TLM. The success of this reaction in describing the inorganic carbon adsorption data is not inconsistent with  $\text{H}_2\text{CO}_3^*$  forming an inner-sphere complex.

The discrepancies in describing the adsorption of dissolved carbonate species on  $\text{Fe}_2\text{O}_3 \cdot \text{H}_2\text{O}(\text{am})$  reflect uncertainty about the bonding environment and the types of surface complexes formed on the oxide surface. This uncertainty is evident in the literature. Potentiometric titration of alumina suspensions indicates that carbonate species are specifically adsorbed (25). Infrared and Raman spectroscopy suggest that the surface complexes contain the carbonate ion in multiple-bonding environments (26). Similarly, infrared analysis of sorbed  $\text{CO}_2(\text{g})$  on hydrated

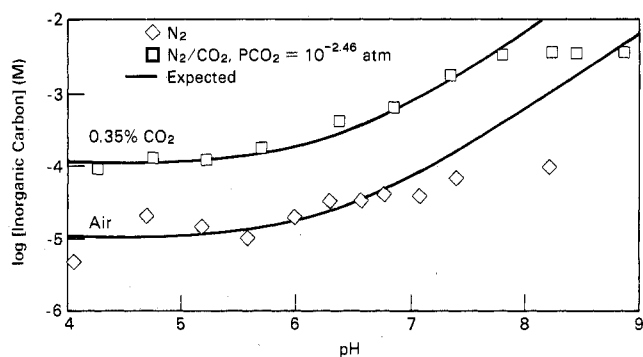


**Figure 3.** Measured inorganic carbon in selected experiments. Solid lines represent expected values in equilibrium with the stated atmospheric composition.

goethite surfaces suggests the formation of both  $\text{HCO}_3^-$  and  $\text{CO}_3^{2-}$  surface complexes (27). The reaction of  $\text{CO}_2(\text{aq})$  with goethite is postulated by Russell et al. (27) to be via coordination of the carbon atom with the triply coordinated oxide ion ( $\text{O}^{2-}$ ) exposed in the (001) groove on the (100) face and subsequent hydrogen bonding of the two oxygen atoms with proximate (A-type) surface hydroxyl groups of the goethite. A  $\text{CO}_3^{2-}$  surface complex is thus formed, which, like phosphate, is especially stable. Additionally, infrared spectroscopy of adsorbed inorganic carbon on freshly precipitated  $\text{Fe}_2\text{O}_3 \cdot \text{H}_2\text{O}(\text{am})$  (28) indicates that the dominant surface complex is the carbonate ion bonded as a unidentate ligand to surface Fe. This evidence, taken collectively, suggests a complex-bonding environment for inorganic carbon species on oxide surfaces. This environment may necessitate different types of surface coordination sites in addition to the single SOH used above.

**Paired-Solute Adsorption. (A) Influence of  $\text{CO}_2(\text{g})$  on  $\text{CrO}_4^{2-}$  Adsorption.** Given the influence of  $\text{CO}_2(\text{aq})$  on  $\text{CrO}_4^{2-}$  adsorption (Figure 1), the total aqueous-phase inorganic carbon  $[C_T]$  was determined for the experimental conditions used in this study. Substantial  $\text{CO}_2(\text{aq})$  remained in the iron suspension under  $\text{N}_2(\text{g})$  despite sparging (Figure 3). Thus,  $\text{CrO}_4^{2-}$  adsorption under an  $\text{N}_2$  atmosphere (Figure 1) is a paired- rather than a single-solute system.

The curves for  $\text{N}_2$  atmosphere in Figure 1 represent the optimum fit to both 0.87 and 17.4 mM  $\text{Fe}_T$  adsorption edges with reactions 7 and 8 in Table II. The surface reactions and the associated adsorption constants derived above for inorganic carbon, along with appropriate  $[C_T]$  data, were included in this optimization. Reactions 5–8 (and associated adsorption constants) were used to describe the  $\text{CrO}_4^{2-}$  adsorption data in Figure 1 with  $P_{\text{CO}_2} = 10^{-2.46}$  atm. These calculations qualitatively predict the shift in adsorption but fail to predict the observed  $\Delta\text{pH}_{50}$ , particularly for the higher iron case; the  $\Delta\text{pH}_{50}$  is the shift in pH at which 50% adsorption occurs relative to the corresponding  $\text{N}_2$  atmosphere edge.

The  $\text{HCO}_3^-$  surface complex reduces  $\text{CrO}_4^{2-}$  adsorption by an electrostatic effect, displacing the edge to lower pH as  $P_{\text{CO}_2}$  increases. Competition between chromate surface complexes and  $\text{H}_2\text{CO}_3^*$  or  $\text{HCO}_3^-$  surface complexes was not found to be significant in model calculations because uncomplexed sites (SOH) are in excess for all experimental conditions in Figure 1. The importance of electrostatic over competitive effects is substantiated by the observation that reaction 5 alone (Table II), which leads to the formation of a charged complex, predicts the same  $\text{CrO}_4^{2-}$   $\Delta\text{pH}_{50}$  as that obtained for reactions 5 and 6. Reaction 6, however, is essential for describing the carbonate adsorption in Figure 2.

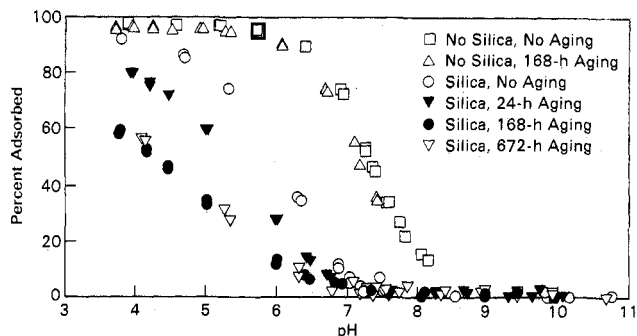


**Figure 4.** Adsorption of  $5.0 \times 10^{-6}$  M  $\text{CrO}_4^{2-}$  on  $\text{Fe}_2\text{O}_3 \cdot \text{H}_2\text{O}(\text{am})$  ( $0.87 \times 10^{-3}$  M  $\text{Fe}_T$ ) in 0.1 M  $\text{NaNO}_3$  under  $\text{N}_2(\text{g})$  atmosphere with and without  $0.71 \times 10^{-3}$  M  $\text{H}_4\text{SiO}_4$ .

The adsorption constants for sulfate and calcium corresponding to reactions 9–11 in Table II were derived from experiments (data not shown) similar to those for  $\text{CrO}_4^{2-}$  adsorption. Inorganic carbon in these experiments was comparable to that in Figure 3. To account for the presence of inorganic carbon, reactions 5 and 6 and carbonate adsorption constants derived above were explicitly included when deriving the sulfate and calcium adsorption constants.

**(B) Influence of Silicic Acid on  $\text{CrO}_4^{2-}$  Adsorption.** Like inorganic carbon,  $\text{H}_4\text{SiO}_4(\text{aq})$  depresses  $\text{CrO}_4^{2-}$  adsorption (Figure 4). The largest reduction in adsorption occurs at pH 6.3, where the adsorption density decreases from 5.60 to 2.00 mmol of Cr/mol of Fe. A larger effect occurs if the  $\text{Fe}_2\text{O}_3 \cdot \text{H}_2\text{O}(\text{am})$  is aged with  $\text{H}_4\text{SiO}_4$  before  $\text{CrO}_4^{2-}$  addition. The aging induces a systematic decrease in  $\text{CrO}_4^{2-}$  adsorption up to 168 h, after which time additional aging up to 672 h has no further influence (Figure 4). In contrast, aging the iron suspension in 0.1 M  $\text{NaNO}_3$  under  $\text{N}_2(\text{g})$  for 168 h does not affect  $\text{CrO}_4^{2-}$  adsorption. This time-dependent reaction of silicic acid with iron reduces the maximum  $\text{CrO}_4^{2-}$  adsorption at pH 4 from 5.5 to 3.5 mmol of Cr/mol of Fe.

The decrease in  $\text{CrO}_4^{2-}$  adsorption induced by  $\text{H}_4\text{SiO}_4$  reflects the adsorption of silica and its effects on the iron surface. Silicic acid has been shown to adsorb strongly on oxide surfaces, with a broad maximum occurring near pH 9 (13, 28–32). Freshly precipitated iron oxides exhibit a high capacity for silicate (33, 34). Silica adsorption alters the surface charge and the  $\text{pH}_{\text{zpc}}$ , as shown by the displacement of alkalimetric titration curves to lower pH values (13). Thus, like  $\text{H}_2\text{CO}_3^*$  (this paper) and  $\text{SO}_4^{2-}$  (5), silica consumes surface sites and forms a charged surface complex that reduces positive interfacial charge and decreases the electrostatic attraction of the  $\text{CrO}_4^{2-}$  anion.

The aging effect with  $\text{H}_4\text{SiO}_4$  reflects silica polymerization in solution or on the iron surface. Depolymerization of monosilicic acid present in the spiking solution may provide a renewable source of reactive monosilicic acid for continuing adsorption up to 168 h. Alternatively, time-dependent polymerization of  $\text{H}_4\text{SiO}_4$  may occur on the  $\text{Fe}_2\text{O}_3 \cdot \text{H}_2\text{O}(\text{am})$ , reducing surface positive charge, changing  $\text{pH}_{\text{zpc}}$ , and covering surface sites active in  $\text{CrO}_4^{2-}$  complexation. Silica substitution in iron oxyhydroxide decreases the oxide  $\text{pH}_{\text{zpc}}$  (35) and selinite adsorption (36). Surface polymerization and multilayer  $\text{H}_4\text{SiO}_4$  adsorption have been observed on both iron and aluminum hydroxide and are influenced by solution pH,  $\text{H}_4\text{SiO}_4$  concentration (29, 31), and surface site saturation.

**(C) Influence of Cations on  $\text{CrO}_4^{2-}$  Adsorption.** The binding of  $\text{CrO}_4^{2-}$  by  $\text{Fe}_2\text{O}_3 \cdot \text{H}_2\text{O}(\text{am})$  was measured separately in the presence of  $\text{K}^+$ ,  $\text{Ca}^{2+}$ , and  $\text{Mg}^{2+}$  to investigate possible enhanced effects of aqueous ion pairing and cation

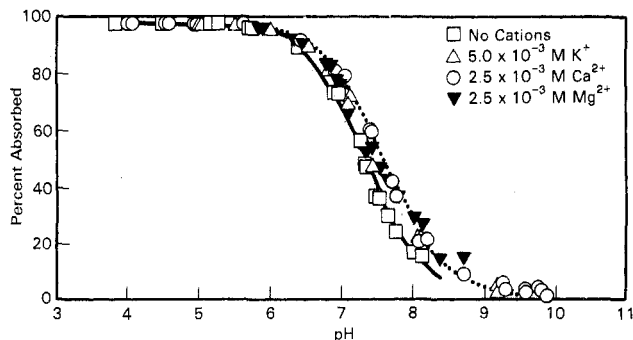


**Figure 5.** Influence of dissolved cations on adsorption of  $5.0 \times 10^{-6}$  M  $\text{CrO}_4^{2-}$  by  $\text{Fe}_2\text{O}_3 \cdot \text{H}_2\text{O}(\text{am})$  ( $0.87 \times 10^{-3}$  M  $\text{Fe}_T$ ) in 0.1 M  $\text{NaNO}_3$ . The solid and dotted lines represent model calculations of  $\text{CrO}_4^{2-}$  adsorption in the absence and presence of  $\text{Ca}^{2+}$ , respectively.

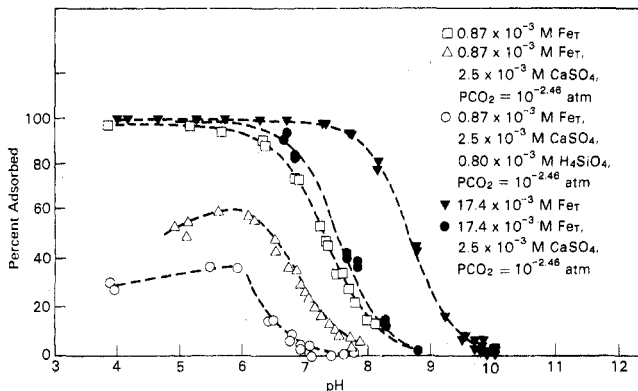


**Figure 6.** Adsorption of  $5.0 \times 10^{-6}$  M  $\text{CrO}_4^{2-}$  on  $\text{Fe}_2\text{O}_3 \cdot \text{H}_2\text{O}(\text{am})$  in 0.1 M  $\text{NaNO}_3$  with and without cosolutes.

adsorption over the 0.1 M  $\text{NaNO}_3$  electrolyte. The cations induce a small increase in  $\text{CrO}_4^{2-}$  binding (Figure 5) above pH 7, where the adsorption of  $\text{CrO}_4^{2-}$  is decreasing as that of the cations is increasing. The divalent cations have a greater effect than  $\text{K}^+$ , in accordance with their higher selectivity for the iron surface (37, 38) over  $\text{Na}^+$ . The increase, however, is slight. The overlap in the adsorption edges of  $\text{CrO}_4^{2-}$ ,  $\text{Ca}^{2+}$ , and  $\text{Mg}^{2+}$  from pH 7 to pH 9 prevents identification of the relative importance of cation adsorption vs.  $\text{CrO}_4^{2-}$  cation-ion pair formation (solution or surface) on the overall retention of Cr(VI).

Calculations with the TLM suggest that the small shift of the Cr(VI) adsorption edge in 0.1 M  $\text{NaNO}_3$  after the addition of  $\text{K}^+$ ,  $\text{Ca}^{2+}$ , and  $\text{Mg}^{2+}$  is consistent with an electrostatic effect induced by cation adsorption. The adsorption of  $\text{CrO}_4^{2-}$  in the presence of  $\text{Ca}^{2+}$  can be described (Figure 5) by reactions 1–8 and 11 in Table II. Calcium adsorption reduces the net negative charge in the double layer over that in 0.1 M  $\text{NaNO}_3$  alone and thus electrostatically encourages additional anion retention. Calculations allowing for the formation of a calcium chromate surface species ( $\text{SOH} + \text{H}^+ + \text{Ca}^{2+} + \text{CrO}_4^{2-} \rightleftharpoons \text{SOH}_2^+ - \text{CrO}_4\text{Ca}^0$ ) do not improve the model simulation. These data suggest that the adsorption of aqueous  $\text{Ca}^{2+} - \text{CrO}_4^{2-}$  ion pairs or their formation on the surface is not significant under these conditions.

**Multiple-Ion Mixtures.** Chromate adsorption is lower in the ion mixture than in the paired-solute systems (Figure 6). The effects of  $\text{CO}_2(\text{g})$ ,  $\text{SO}_4^{2-}$ , and  $\text{H}_4\text{SiO}_4$  on  $\text{CrO}_4^{2-}$  adsorption in the mixture are qualitatively additive. The small enhancement of  $\text{CrO}_4^{2-}$  adsorption induced by  $\text{Ca}^{2+}$  is significant when compared to the effects of the major anions. Sulfate and  $\text{H}_4\text{SiO}_4$  dominate the downward displacement of the adsorption edge in the ion mixture, with  $\text{SO}_4^{2-}$  inducing site saturation in the low-iron case below pH 6.2. Site saturation occurs when adsorbing ions



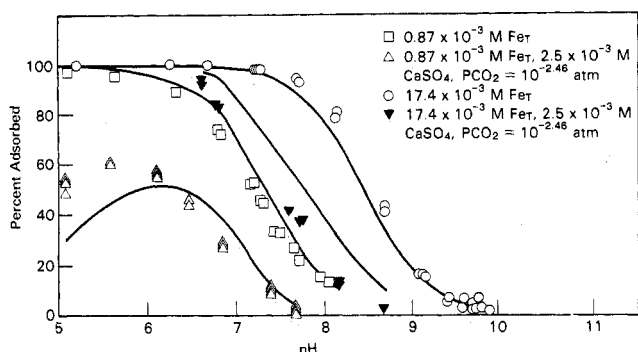


**Figure 7.** Adsorption modeling of  $5.0 \times 10^{-6}$  M  $\text{CrO}_4^{2-}$  on  $\text{Fe}_2\text{O}_3 \cdot \text{H}_2\text{O}(\text{am})$  in 0.1 M  $\text{NaNO}_3$  with and without cosolutes. Solid lines are model calculations.

significantly reduce the number of uncomplexed surface sites (SOH) and adsorption does not reach 100% at its maximum. Silicic acid has a large influence on  $\text{CrO}_4^{2-}$  adsorption in the mixture below pH 8. When higher levels of iron oxyhydroxide ( $17.4 \times 10^{-3}$  M) are used with the same solute concentrations, the adsorption edge for the multiple-solute system is displaced to lower pH relative to the edge for  $\text{CrO}_4^{2-}$  as a single adsorbate, but site saturation does not occur within the experimental pH range (pH  $\geq 6.7$ ) (Figure 6). Under these conditions, the adsorption of  $\text{CrO}_4^{2-}$  from the mixture approaches 100%, but the adsorption is displaced ( $\Delta\text{pH}_{50} = 1.20$ ) to the left of its single-solute edge. The influence of inorganic carbon on  $\text{CrO}_4^{2-}$  adsorption becomes of increasing importance above pH 8.5, because the concentrations of total dissolved carbon are relatively high ( $[\text{C}_\text{T}] = 10^{-1.3}$  M).

The aqueous concentration of  $\text{SO}_4^{2-}$  changes in the multiple-solute experiments through adsorption. Inorganic carbon is also adsorbed but is maintained at constant activity by gas-phase equilibrium. Equilibrium  $\text{SO}_4^{2-}$  concentrations were observed to differ between the high- and low-iron cases with a greater removal occurring with more iron. Site saturation may well have occurred in the high-iron case if major ion concentrations were held constant or if high-iron experiments were conducted at pH values (e.g., pH 5–6) where saturation occurred in the low-iron experiments.

Chromate adsorption in the multiple-ion mixture was calculated with the adsorption constants in Table II (see Figure 7). The constants provide excellent simulation of the adsorption edge for the low-iron case but underestimate  $\text{CrO}_4^{2-}$  adsorption below pH 6 where  $\text{SO}_4^{2-}$  is inducing site saturation. For the high-iron case, the calculation describes the shape but not the location of the edge, overestimating  $\text{CrO}_4^{2-}$  adsorption by as much as 15%. This overestimate would be reduced if the formation of a  $\text{CO}_3^{2-}$  surface complex is included.

Surface speciation of  $\text{Fe}_2\text{O}_3 \cdot \text{H}_2\text{O}(\text{am})$  in the multiple-ion mixture was calculated as a function of pH with the TLM. In the high-iron case, reactive surface sites (SOH) remain in excess within the experimental range of pH (6.7–8.8) in spite of the adsorption of major ions in solution. In the absence of competition for a subset of surface sites, the shift in the edge between the two high-iron curves (Figure 7) arises from a reduction in interfacial charge imposed by the surface complexation of  $\text{SO}_4^{2-}$  and dissolved  $\text{CO}_2(\text{g})$ . The reduced positive charge decreases the electrostatic attraction for all negatively charged ions, including  $\text{CrO}_4^{2-}$ . However, site saturation occurs in the low-iron case (Figure 8) below pH 6.2. That is, the total concentration of uncomplexed neutral sites (SOH) drops with pH, and competition occurs among all reactive species for a limited number of sites. The resulting position and shape of the

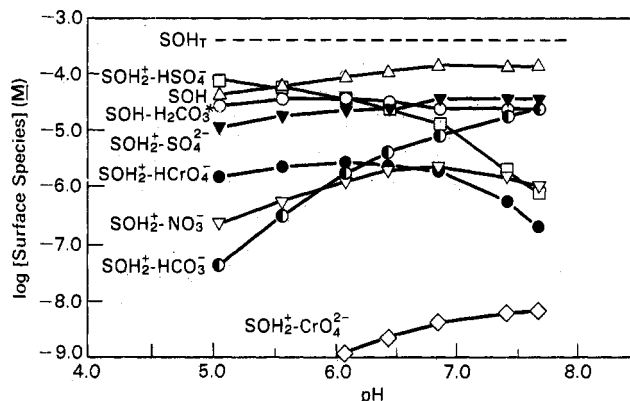


**Figure 8.** Calculated surface speciation of  $\text{Fe}_2\text{O}_3 \cdot \text{H}_2\text{O}(\text{am})$  ( $0.87 \times 10^{-3}$  M  $\text{Fe}_\text{T}$ ) in the presence of  $5.0 \times 10^{-6}$  M  $\text{CrO}_4^{2-}$ ,  $2.5 \times 10^{-3}$  M  $\text{CaSO}_4(\text{aq})$ , 0.1 M  $\text{NaNO}_3$ , and  $P_{\text{CO}_2} = 2.46$  atm. The total number of surface sites corresponding to the iron concentration is designated  $[\text{SOH}_\text{T}]$  ( $\log [\text{SOH}_\text{T}] = -3.36$  mol/L).

edge are controlled by both surface electrostatics and site selectivity. The surface speciation calculations also show that  $\text{NO}_3^-$  is an important surface species; the high electrolyte concentration drives  $\text{NO}_3^-$  to the surface in spite of its low complexation constant (Table II).

### Summary

Major groundwater anions bind to the surface of  $\text{Fe}_2\text{O}_3 \cdot \text{H}_2\text{O}(\text{am})$ , reduce positive charge, and compete directly with  $\text{CrO}_4^{2-}$  as sites become limited. The surface reaction of these anions reduces  $\text{CrO}_4^{2-}$  adsorption. In ion mixtures with solute concentrations typical of the subsurface (39, 40),  $\text{CrO}_4^{2-}$  adsorption is suppressed 50%–80% over that in weakly interacting electrolyte. Cations have little influence on  $\text{CrO}_4^{2-}$  adsorption, indicating that ion pair formation in solution or on the surface is not of consequence.

Diffuse double-layer model simulations using single-solute adsorption constants are in good agreement with the experimental data from the multiple-ion mixture. Similarly, the adsorption of heavy metals (Cd, Pb, and Zn) on goethite in synthetic seawater has been simulated with reasonable accuracy by using single-solute intrinsic adsorption constants (38). However, other calculations suggest that site heterogeneity and possibly multiple-site adsorption behavior must be considered to quantitatively simulate competition between strongly adsorbing anions (41).

Chromate adsorption in the subsurface environment may be significantly suppressed by the presence of common anionic constituents in groundwater. Elevated levels of dissolved  $\text{CO}_2(\text{g})$ ,  $\text{H}_4\text{SiO}_4$ , and  $\text{SO}_4^{2-}$  may all dramatically reduce  $\text{CrO}_4^{2-}$  adsorption. Surface complexation constants corrected for the influence of surface charging can be used along with diffuse double-layer models of adsorption to estimate the extent of suppression anticipated under various subsurface chemical regimes.

**Registry No.**  $\text{CrO}_4^{2-}$ , 13907-45-4;  $\text{Fe}_2\text{O}_3$ , 1309-37-1;  $\text{CO}_2$ , 124-38-9;  $\text{H}_4\text{SiO}_4$ , 10193-36-9;  $\text{K}^+$ , 24203-36-9;  $\text{Ca}^{2+}$ , 14127-61-8;  $\text{Mg}^{2+}$ , 22537-22-0.

### Literature Cited

- U.S. Environmental Protection Agency *Review of the Environmental Effects of Pollutants*; U.S. Government Printing Office: Washington, DC, 1978; Vol. III, EPA 600/1-78-023.
- U.S. Environmental Protection Agency *Quality Criteria for Water*; U.S. Government Printing Office: Washington, DC, 1976; EPA 440/9-76-023.
- Griffin, R. A.; Au, A. K.; Frost, R. R. *J. Environ. Sci. Health, Part A* 1977, *A12*, 431–449.

- (4) MacNaughton, M. G. In *Biological Implications of Metals in the Environment*; Drucker, H.; Wildung, R. E., Eds.; National Technical Information Service: Springfield, VA, 1977; pp 240-253; CONF-750929.
- (5) Leckie, J. O.; Benjamin, M. M.; Hayes, K.; Kaufman, G.; Altman, S. *Adsorption/Coprecipitation of Trace Elements from Water with Iron Oxyhydroxide*; Electric Power Research Institute: Palo Alto, CA, 1980; EPRI-RP-910.
- (6) Davis, J. A.; Leckie, J. O. *J. Colloid Interface Sci.* **1980**, *74*, 32-43.
- (7) Mayer, L. M.; Schick, L. L. *Environ. Sci. Technol.* **1981**, *15*, 1482-1484.
- (8) Artioli, J.; Fuller, W. H. *J. Environ. Qual.* **1979**, *8*, 503-510.
- (9) Stollenwerk, K. G.; Grove, D. B. *J. Environ. Qual.* **1985**, *14*, 150-155.
- (10) Robertson, F. N. *Ground Water* **1975**, *13*, 516-527.
- (11) Hingston, F. J.; Posner, A. M.; Quirk, J. P. *Discuss. Faraday Soc.* **1971**, *52*, 234-242.
- (12) Stumm, W.; Kummert, R.; Sigg, L. *Croat. Chem. Acta* **1980**, *53*, 291-312.
- (13) Sigg, L.; Stumm, W. *Colloids Surf.* **1980**, *2*, 101-117.
- (14) Davis, J. A.; James, R. O.; Leckie, J. O. *J. Colloid Interface Sci.* **1978**, *63*, 480-499.
- (15) Girvin, D. C.; Ames, L. L.; McGarrah, J. E. *Neptunium Adsorption on Synthetic Amorphous Iron Oxyhydroxide*; Pacific Northwest Laboratory: Richland, WA, Nov. 1984; PNL-SA-11229.
- (16) Westall, J. *FITEQL: A Computer Program for Determination of Chemical Equilibrium Constants from Experimental Data*; Department of Chemistry, Oregon State University: Corvallis, OR, 1982; Report 82-01.
- (17) Stumm, W.; Morgan, J. J. *Aquatic Chemistry*; Wiley: New York, 1981.
- (18) Truesdell, A. H.; Jones, B. F. *J. Res. U.S. Geol. Surv.* **1974**, *2*, 233-248.
- (19) Ball, J. W.; Nordstrom, D. K.; Jenne, E. A. *Additional and Revised Thermochemical Data and Computer Code for WATEQ2—A Computerized Chemical Model for Trace and Major Element Speciation and Mineral Equilibria of Natural Waters*; U.S. Geological Survey: Menlo Park, CA, 1980; Water Resources Investigations 78-116.
- (20) Ball, J. W.; Jenne, E. A.; Cantrell, M. W. *WATEQ3: A Geochemical Model with Uranium Added*; U.S. Geological Survey: Menlo Park, CA, 1981; Open-File Report 81-1183.
- (21) Krupka, K. M.; Jenne, E. A. *WATEQ3 Geochemical Model: Thermodynamic Data for Several Additional Solids*; Pacific Northwest Laboratory: Richland, WA, 1982; PNL-4276.
- (22) Baes, C. F., Jr.; Mesmer, R. E. *The Hydrolysis of Cations*; Wiley-Interscience: New York, 1976.
- (23) Schmidt, R. L. *Thermodynamic Properties and Environmental Chemistry of Chromium*; Pacific Northwest Laboratory: Richland, WA, 1984; PNL-4881.
- (24) Choi, W. W.; Chen, K. Y. *Environ. Sci. Technol.* **1979**, *13*, 189-196.
- (25) Feldkamp, J. R.; Shah, D. N.; Meyer, S. L.; White, J. L.; Hem, S. L. *J. Pharm. Sci.* **1981**, *70*, 638-640.
- (26) White, J. L.; Hem, S. L. *J. Pharm. Sci.* **1975**, *64*, 468-469.
- (27) Russell, J. D.; Patterson, E.; Fraser, A. R.; Farmer, V. C. *J. Chem. Soc., Faraday Trans. 1* **1975**, *71*, 1623-1630.
- (28) Harrison, J. B.; Berkheiser, V. E. *Clays Clay Miner.* **1982**, *30*, 97-102.
- (29) Hingston, F. J.; Raupach, M. *Aust. J. Soil Res.* **1967**, *5*, 295-309.
- (30) Beckwith, R. S.; Reeve, R. *Aust. J. Soil Res.* **1963**, *1*, 157-168.
- (31) Yokoyama, T.; Nakazato, T.; Tarantani, T. *Bull. Chem. Soc. Jpn.* **1980**, *53*, 850-853.
- (32) Hingston, F. J.; Posner, A. M.; Quirk, J. P. *J. Soil Sci.* **1972**, *23*, 177-192.
- (33) McPhail, M.; Page, A. L.; Bingham, F. T. *Soil Sci. Soc. Am. Proc.* **1972**, *36*, 510-514.
- (34) McKeague, J. A.; Cline, M. G. *Can. J. Soil Sci.* **1963**, *43*, 83-96.
- (35) Pyman, M. A.; Bowden, J. W.; Posner, A. M. *Clay Miner.* **1979**, *14*, 87-92.
- (36) Anderson, P. R.; Benjamin, M. M. *Environ. Sci. Technol.* **1985**, *19*, 1048-1053.
- (37) Davis, J. A.; Leckie, J. O. *J. Colloid Interface Sci.* **1978**, *67*, 90-107.
- (38) Balistrieri, L. S.; Murray, J. W. *Geochim. Cosmochim. Acta* **1982**, *46*, 253-265.
- (39) Hem, J. D. *U.S. Geol. Surv. Water-Supply Pap.* **1970**, No. 1473.
- (40) Harmon, R. S.; White, W. B.; Drake, J. J.; Hess, J. W. *Water Resour. Res.* **1975**, *11*, 963-967.
- (41) Goldberg, S. *Soil Sci. Soc. Am. J.* **1985**, *49*, 851-856.

Received for review May 7, 1986. Accepted February 6, 1987. This research was funded by the Electric Power Research Institute, Inc. (EPRI), under Contract RP2485-03, "Chemical Attenuation Studies".